Regulation of branchial V-H$^+$-ATPase, Na$^+$/K$^+$-ATPase and NHE2 in response to acid and base infusions in the Pacific spiny dogfish (*Squalus acanthias*)

Martin Tresguerres*, Fumi Katoh, Heather Fenton, Edyta Jasinska and Greg G. Goss

Dept of Biological Sciences, University of Alberta, Edmonton, Alberta T5G 2E9, Canada and *Bamfield Marine Research Centre, Bamfield, BC V0R 1B0, Canada*

*Author for correspondence (e-mail: martint@ualberta.ca)

Summary

To study the mechanisms of branchial acid–base regulation, Pacific spiny dogfish were infused intravenously for 24 h with either HCl (495± 79 μmol kg^{-1} h^{-1}) or NaHCO$_3$ (981±235 μmol kg^{-1} h^{-1}). Infusion of HCl produced a transient reduction in blood pH. Despite continued infusion of acid, pH returned to normal by 12 h. Infusion of NaHCO$_3$ resulted in a new steady-state acid–base status at ~0.3 pH units higher than the controls. Immunostained serial sections of gill revealed the presence of separate vacuolar proton ATPase (V-H$^+$-ATPase)-rich or sodium-potassium ATPase (Na$^+$/K$^+$-ATPase)-rich cells in all fish examined. A minority of the cells also labeled positive for both transporters. Gill cell membranes prepared from NaHCO$_3$-infused fish showed significant increases in both V-H$^+$-ATPase abundance (300±81%) and activity. In addition, we found that V-H$^+$-ATPase subcellular localization was mainly cytoplasmic in control and HCl-infused fish, while NaHCO$_3$-infused fish demonstrated a distinctly basolateral staining pattern. Western analysis in gill membranes from HCl-infused fish also revealed increased abundance of Na$^+$/H$^+$ exchanger 2 (213±5%) and Na$^+$/K$^+$-ATPase (315±88%) compared to the control.

Key words: dogfish, *Squalus acanthias*, gill, acid–base regulation, H$^+$-ATPase, Na$^+$/K$^+$-ATPase, NHE, acid infusion, base infusion, alkalosis, acidosis.

Introduction

The gills of marine elasmobranchs are an excellent model for studying the acid–base regulatory mechanism of fishes. While they are the principal acid–base regulatory organs (Heisler, 1988), they also have a substantial advantage relative to the gills of teleosts in that ion secretion principally takes place in the rectal gland (Shuttleworth, 1988). This eliminates ion secretion as one potentially confusing factor when studying branchial ionic transfers for acid–base regulation. Despite these advantages, the underlying cellular mechanisms for acid–base regulation are far from being fully understood.

For branchial acid secretion in marine elasmobranchs two mechanisms have been proposed. The first involves extrusion of protons in electroneutral exchange for environmental sodium (i.e. *via* Na$^+$/H$^+$ exchangers; NHEs) and the second is *via* secretion of protons by a vacuolar-type proton ATPase (H$^+$-ATPase). At first sight, the former has the advantage of being energetically less expensive, because it would take advantage of the inward directed sodium gradient to drive proton secretion. The proposed apical transporters are members of the NHE family, homologous to the mammalian NHE2 and NHE3. These transporters would be localized in the same cells as the enzyme sodium-potassium ATPase (Na$^+$/K$^+$-ATPase) (see Claiborne et al., 2002). The second hypothesis is based on the description of H$^+$-ATPase in the gills of *Squalus acanthias* by Wilson et al. (1997). However, the relationship between this transporter and acid secretion are based only on the subapical localization, and an analogy to the α-secreting cells of the mammalian collecting duct, the frog skin and the turtle urinary bladder (Brown and Breton, 1996; Kirschner, 2004). Recently, the H$^+$-ATPase has also been proposed to be involved in base secretion in a euryhaline elasmobranch, the Atlantic stingray *Dasyatis sabina* (Piermarini and Evans, 2001). These authors found strong cytoplasmic H$^+$-ATPase staining in cells that were not labeled for Na$^+$/K$^+$-ATPase. They proposed that H$^+$-ATPase stored in vesicles could be recruited to the basolateral membrane under alkalotic stress, but this hypothesis was not investigated further. Demonstration of cellular remodeling and basolateral localization following alkalotic stress would support their hypothesis that these cells are involved in base secretion, in an analogous way to the β-type intercalated cells in the mammalian collecting duct and turtle urinary bladder. However, the Atlantic stingray is a euryhaline myliobatiform, and this model might differ from the one present in exclusively marine elasmobranchs.

The objective of this study was to examine the involvement of H$^+$-ATPase, Na$^+$/K$^+$-ATPase and NHE2 in the branchial acid–base regulatory mechanism of the dogfish, *Squalus acanthias*. In order to exacerbate the signals, we infused the

fish with acid and base solutions for 24 h. Our results support the role of NHE2 in acid secretion and indicate that increases in H⁺-ATPase abundance and activity, as well as a change in its subcellular localization, are required for upregulation of base secretion.

Materials and methods
Animals

Pacific spiny dogfish (*Squalus acanthias* L) were obtained from commercial fishermen, and held in a 288 m³ tank provided with flowing seawater (11°C, 31 ppt salinity) at the Bamfield Marine Research Centre (British Columbia, Canada). Fish were fed twice per week with flounder and squid while being housed in this tank. They were not fed following removal from the tank.

Antibodies and reagents

Rabbit anti-NHE2 antibody was kindly provided by Dr Mark Donowitz (National Institutes of Health, Bethesda, Maryland, MD, USA). This antibody was designed against 87 amino acids of the C-terminal region of mammalian NHE2, so the protein we detected should be regarded, throughout the text, as a NHE2-like protein (NHE2-lp). This antibody has been successfully used to detect NHE2-lp in elasmobranchs (Edwards et al., 2002). Rabbit anti-Na⁺/K⁺-ATPase antibody was raised against a synthetic peptide corresponding to a part of a highly conserved region of the α-subunit (Katoh et al., 2000; Katoh and Kaneko, 2003). Rabbit anti-H⁺-ATPase was raised against a synthetic peptide based on the highly conserved and hydrophilic region in the A-subunit (Katoh et al., 2003). A donkey anti-rabbit fluorescent secondary antibody (Li-Cor Inc., Lincoln, NE, USA) was used for western analysis. We were unable to run pre-absorption controls because the corresponding proteins were not available. However, in the western analyses we always found very distinct bands of about the expected molecular masses for all the antibodies tested. Together with the absence of signal in nitrocellulose membranes incubated with blocking buffer without the primary antibody, it suggests that the antibodies used have an acceptable specificity.

Unless otherwise mentioned, the reagents used in this study were purchased from Sigma (St Louis, MO, USA).

Surgery and acid–base infusions

A total of 16 animals (2.28±0.31 kg) were removed from the housing tank and cannulated for this study. We used fish of equivalent sizes to standardize infusion rates. Fish were caught by hand, anesthetized with MS-222 (1:10000), and transferred to an operating table, where the gills were irrigated with aerated seawater containing MS-222. Two cannulae (PE-50, Clay-Adams, Parsippany, NJ, USA) were fitted into the caudal vein and artery. The incision was sutured with stitches and a small volume of a heparanized (50 i.u. ml⁻¹ Na⁺-heparin) 500 mmol l⁻¹ NaCl solution was injected before blocking the end of the tubing with a pin. The animals were transferred to experimental boxes (36 l) with aerated flowing seawater. After a 24 h recovery period, the venous cannula was connected to a Gilson miniplus peristaltic pump (Middleton, WI, USA) and the experimental solution was infused at a rate of 4.04±0.83 ml h⁻¹ kg⁻¹. The arterial cannula allowed us to obtain blood samples during the course of the experiment.

In order to induce acidosis or alkalosis in the blood, fish were infused with either 125 mmol l⁻¹ HCl or 250 mmol l⁻¹ NaHCO₃ to achieve nominal H⁺ and HCO₃⁻ infusion rates of 500 and 1000 µmol kg⁻¹ h⁻¹. The actual acid and base loads were 495±79 and 981±235 µmol kg⁻¹ h⁻¹, respectively. These concentrations were selected after previous trial experiments and reference to other published work (Gilmour et al., 2001; Wood et al., 1995). Infusion of acid at a nominal rate of 1000 µmol. kg⁻¹ h⁻¹ in early experiments proved to be fatal after ~6 h, possibly as a result of haemolysis.

To minimize osmotic disturbances, the osmolarity of the infusion solutions was adjusted to 1000 mOsm with the addition of NaCl. Animals infused with 500 mmol l⁻¹ NaCl served as control. Table 1 shows the base, acid and NaCl load in each of the treatments. In addition, four other animals were subjected to surgery, but no cannula was inserted into the caudal vein or artery. These fish represented the sham-operated group, and they were otherwise treated exactly the same as the experimental fish.

Blood samples

Arterial blood samples (300 µl) were taken at times 0, 1, 3, 6, 12 and 24 h. After the blood extraction, an equal volume of heparanized 500 mmol l⁻¹ NaCl solution was injected into the fish to minimize changes in blood volume and prevent clotting. Blood samples were used for haematocrit analysis (~50 µl) and pH determination (~80 µl). The rest of the sample was centrifuged at 12 000 *g* and plasma osmolarity and total CO₂ were measured immediately. The remaining plasma was preserved at –80°C for later sodium and chloride concentrations assays.

Analytical procedures on plasma samples

Osmolarity was measured with a micro osmometer (Precision Systems Inc., Natick, MA, USA). A pH-sensitive electrode (Radiometer, Copenhagen, Denmark) was used to measure blood pH. The total CO₂ content was determined in a Cameron chamber equipped with a CO₂ electrode (Radiometer, Copenhagen). Na⁺ concentration was read by flame spectrometry (Perkin-Elmer model 3300, Norwalk, CT,

Table 1. *Acid, base and NaCl infusion rates in each of the treatments*

Infusion	H⁺	HCO₃⁻	Na⁺	Cl⁻
250 mmol l⁻¹ HCO₃⁻	–	981±235	1962±470	981±235
125 mmol l⁻¹ HCl	495±79	–	1484±237	1978±317
500 mmol l⁻¹ NaCl	–	–	1832±128	1832±128

The values are expressed as mequiv kg⁻¹ h⁻¹, *N*=4.

USA). Cl⁻ concentration was measured by the mercuric thiocyanate method (Zall et al., 1956).

Terminal sampling

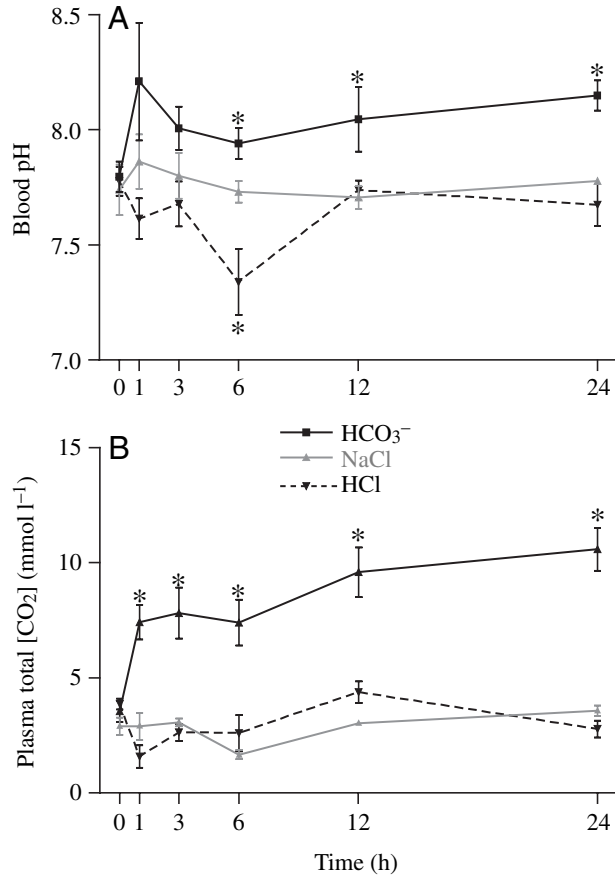After 0 (sham) or 24 h of infusion, fish were killed by

injection of 3 ml of a saturated KCl solution. Samples of gill were excised and snap-frozen in liquid nitrogen for later western blot and ATPase analyses. Other gill samples were immersed in fixative for immunohistochemistry and electron microscopy (see below).

Immunohistochemistry

Gill samples for immunohistochemistry were fixed in 3% paraformaldehyde, 0.1 mol l⁻¹ cacodylate buffer (pH 7.4) for 6 h at 4°C and dehydrated in a graded ethanol series. After embedding in paraffin, 4 μm sections were cut from gill filaments. Sections from the trailing and leading edges, as well as from the middle portion of the filament, were placed in glycerol-albumin (Mayer's fixative)-coated slides (1 section per slide). Sections were deparaffinized in toluene, hydrated in a decreasing ethanol series, washed in double distilled water (ddH₂O), and then exposed to 0.6% H₂O₂ for 30 min to devitalize endogenous peroxidase activity. After blocking with

Fig. 1. Blood parameters of fish infused intravenously with either 125 mmol l⁻¹ HCl (495±79 μmol kg⁻¹ h⁻¹), 250 mmol l⁻¹ NaHCO₃ (981±235 μmol kg⁻¹ h⁻¹) or 500 mmol l⁻¹ NaCl (1832± 128 μmol kg⁻¹ h⁻¹) (mean ± S.E.M., N=4). (A) Arterial blood pH. (B) Total [CO₂] in plasma from arterial blood samples. *P<0.05 compared to the control value (NaCl) of the respective time (RM-ANOVA, one-way ANOVA, Dunnet's *post* test).

Table 2. *Parameters in blood or plasma of the experimental fish at the sampling times*

Time (h)	Haematocrit (%)	[Na⁺] (mmol l⁻¹)	[Cl⁻] (mmol l⁻¹)	Osmolarity (mOsm l⁻¹)
0	15.2±2.5	246.5±2.6	273.7±8.4	968.8±0.9
1	15.1±2.1	256.8±5.6	275.9±4.3	973.0±4.0
3	14.7±2.4	247.0±7.5	282.0±2.1	979.1±8.1
6	13.9±2.2	259.3±4.5	279.7±4.8	958.8±7.8
12	13.3±2.5	247.2±7.2	260.5±2.4	956.9±3.4
24	12.6±2.3	239.2±11.1	266.8±11.1	960.2±8.1

Values are means ± S.E.M. (N=12) from the combination of NaCl-, acid- and base-infused fish at each time. There were no significant differences between sampling times or treatments.
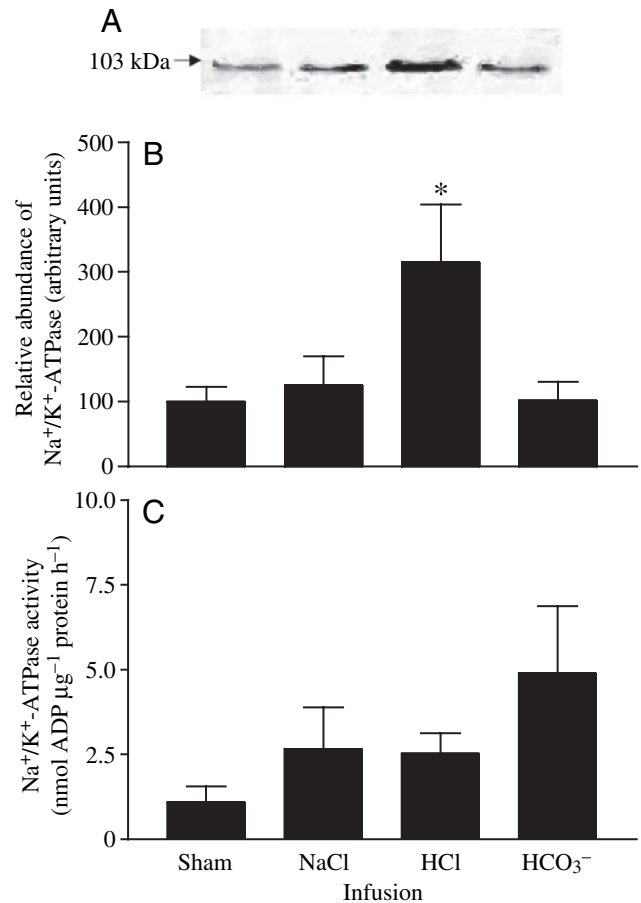

Fig. 2. Na⁺/K⁺-ATPase in the membrane fraction of the gills of sham-operated, NaCl-, acid- and base-infused fish. (A) Representative quantitative immunoblotting against the α-subunit of the Na⁺/K⁺-ATPase: a distinct band of ~102.8 kDa was obtained. (B) Fluorometric analysis revealed that Na⁺/K⁺-ATPase abundance in acid-infused fish increased to 315±88% of sham-operated fish (100±22%; N=4). (C) Na⁺/K⁺-ATPase activity. Values are mean ± S.E.M., N=4. No significant differences were found among treatments. *P<0.05 (one-way ANOVA, Dunnet's *post* test).
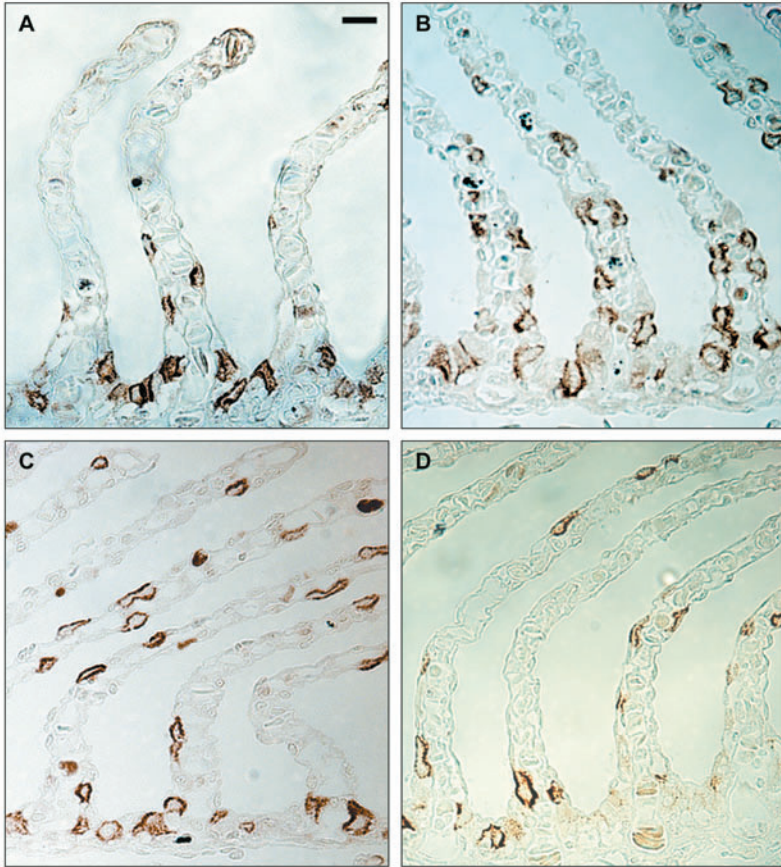
Fig. 3. Representative images of Na$^+$/K$^+$-ATPase immunostaining in gills from sham-operated (A), acid-infused (B), base-infused (C) and NaCl-infused (D) fish. The sections were from equivalent regions in the gill filament, near the trailing edge. Note the greater number of labeled cells in the lamellae in B and C. Scale bar, 10 μm.

2% normal goat serum (NGS) for 30 min, the sections were incubated overnight at 4°C with the respective antibody, which was diluted in 2% NGS, 0.1% bovine serum albumin, 0.02% limpet haemocyanin, 0.01% NaN$_3$ in 10 mmol l^{-1} PBS, pH 7.4. The anti-Na$^+$/K$^+$-ATPase antibody was diluted 1:4000, and the antibody against the A-subunit of the H$^+$-ATPase was diluted 1:1000. In order to look for colocalization of the transporters, consecutive sections were incubated with different antibodies. The next steps were performed at room temperature, using the Vectastain ABC kit (Vector Laboratories, CA, USA) as follows. Sections were incubated with a biotinylated goat anti-

rabbit secondary antibody for 30 min and then incubated with a horseradish peroxidase-labeled streptavidin solution for 1 h. Sections were rinsed in ddH$_2$O for 6 min and then in phosphate-buffered saline (PBS) for 2 min inbetween incubations. Bound antibodies was visualized by soaking the sections in a solution containing 20% w/v 3,3′-diaminobenzidine tetrahydrochloride (DAB) and 0.005% H$_2$O$_2$ in 50 mmol l^{-1} Tris-buffered saline, pH 7.6. DAB reacts with the horseradish peroxidase, producing a brown coloration. As controls, gill sections from every fish were incubated without any primary antibody. These sections never showed specific staining, regardless of the treatment and location in the gill (trailing or leading edge of the filament). The qualitative description of the amount of positively labeled cells is based on three pairs of sections from the leading edge, three pairs of sections from the approximate middle of the filament, and three pair of sections from the trailing edge. Each pair of sections contained one section labeled for Na$^+$/K$^+$-ATPase and the other for H$^+$-ATPase. A minimum of two filaments per fish, and three fish per treatment were analyzed.

Transmission electron microscopy

Gill samples for transmission electron microscopy (TEM) were fixed in 1.5% glutaraldehyde, 3% paraformaldehyde, 0.1 mol l^{-1} cacodylate buffer (pH 7.4) for 6 h at 4°C, immersed in 50% ethanol for 2 h and stored in 70% ethanol at 4°C. Samples were rehydrated after arrival to Edmonton, post-fixed in 2% OsO$_4$ for 2 h, dehydrated in an ethanol graded series, transferred to propylene oxide and embedded in Epon resin. Ultrathin sections (~90 nm) were cut with an automatic microtome (Reichert Ultracut E), mounted in copper grids, counter stained with 1% uranyl acetate (1 h) and 0.02% lead citrate (1 min), and observed using a TEM (Philips model 201).

Western blot analysis

Frozen gill samples were weighed, immersed in liquid nitrogen and pulverized in a porcelain grinder. The resultant powder was resuspended in 1:10 w/v of ice-cold homogenization buffer (250 mmol l^{-1} sucrose, 1 mmol l^{-1} EDTA, 30 mmol l^{-1} Tris, 100 mg ml^{-1} PMSF and 2 mg ml^{-1} pepstatin, pH 7.4) and sonicated on ice for 20 s. Debris was removed by two low speed centrifugations (3000 g for 5 min, 4°C) and gill membranes were pelleted by a final high
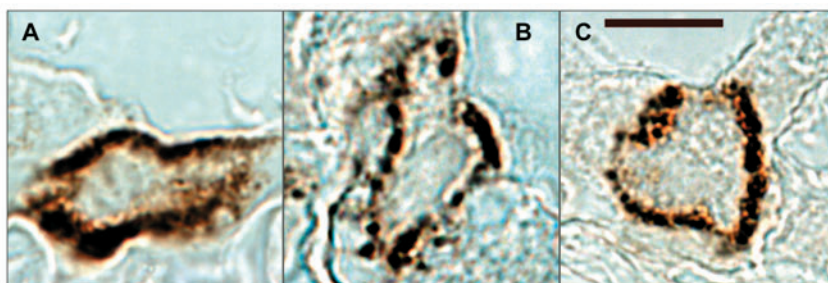

Fig. 4. High magnification micrographs showing the Na$^+$/K$^+$-ATPase subcellular localization in control (A), acid- (B) and base-infused (C) fish. Note that the immunostaining is basolateral in all cases. Scale bar, 10 μm.

speed centrifugation (20 800 g for 30 min, 4°C). The resulting pellets were resuspended in homogenization buffer and a sample was saved for protein determination analysis (BCA protein assay reagent kit, Pierce, IL, USA), which was performed in triplicate. The remaining sample was combined with 2× Laemmli buffer (Laemmli, 1970) for western analysis. 30 μg (for NHE2) or 50 μg (for H$^+$-ATPase) of total protein were separated in a 7.5% polyacrylamide mini-gel (45 min at 180 V) and transferred to a nitrocellulose (NC) membrane using a semi-dry transfer cell (Bio-Rad Laboratories, Inc., USA). Following blocking (5% chicken ovoalbumin in 0.5 mol l^{-1} Tris-buffered saline (TBS) with 0.1% Triton X-100, pH 8.0, overnight at 4°C), the NC membranes were incubated with primary antibodies against either the A-subunit of the H$^+$-ATPase or NHE2 (1:2500 in blocking buffer) with gentle rocking at 4°C overnight. After four washes with TBS–Triton X-100 (0.2%), the NC membrane was blocked briefly for 15 min and incubated with the fluorescent secondary antibody (4°C overnight). Bands were visualized and quantified using the Odyssey infra-red imaging system and software (Li-Cor Inc.), which allows direct linear quantification of western blots. After quantification, NC membranes probed against H$^+$-ATPase were soaked in stripping buffer (50 mmol l^{-1} Tris, pH 8.0, 1% SDS, 0.7% β-mercaptoethanol) for 30 min at 60°C to remove the previously used antibodies. After stripping, NC membranes were washed three times with TBS-Triton X-100 (0.2%) (20 min each), blocked for 15 min, and incubated with the primary antibody against Na$^+$/K$^+$-ATPase following the protocol described above. To correct for differences in loading, protein concentration in each lane was quantified after staining with Coomassie Brilliant Blue. Hence, the amount of H$^+$-ATPase, Na$^+$/K$^+$-ATPase and NHE2 in each sample was given by the ratio of antibody/Coomassie Blue fluorescence. Values are presented relative to the samples from sham-operated fish in each gel. Membranes incubated with blocking buffer without the primary antibody served as controls. These membranes did not show any labeling.

ATPase assays

Gill membranes were obtained as described above, with the difference that homogenization was performed in ice-cold SEID buffer (200 mmol l^{-1} sucrose, 20 mmol l^{-1} Na$_2$EDTA, 40 mmol l^{-1} imidazole, 0.5% Na$^+$-deoxycholic acid; McCormick, 1993). Homogenate (10 μl) from each sample was added to nine wells in a 96-well plate. This provided three treatments for each sample: control, ouabain (500 μmol l^{-1}) and ouabain (500 μmol l^{-1}) + bafilomicyn (50 nmol l^{-1}), with triplicate measurements of each treatment. Na$^+$/K$^+$-ATPase activity was obtained by subtracting the ouabain-treated ATPase activity from control ATPase activity (see McCormick, 1993). H$^+$-ATPase activity was assessed by calculating the difference in ATPase activity between the ouabain- and the ouabain + bafilomycin-treated, as described by Hawkings et al. (2004). Protein concentration in each well was determined (Pierce, IL, USA) after evaporation of the assay solution (60°C overnight).
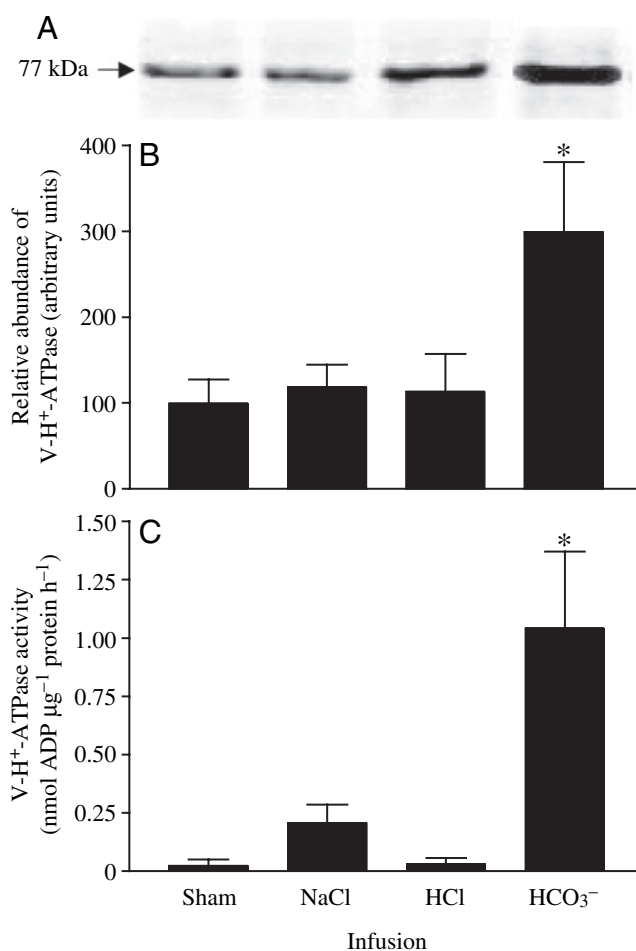

Fig. 5. V-H$^+$-ATPase in the membrane fraction of gills of sham-operated, NaCl-, acid- and base-infused fish. (A) Representative quantitative immunoblotting against the A-subunit of the V-H$^+$-ATPase: a distinct band of ~77 kDa was obtained. (B) Fluorometric analysis revealed that the abundance of the A-subunit of the V-H$^+$-ATPase in base-infused fish increased to 300±81% of sham-operated fish (100±28%) (N=4). (C) V-H$^+$-ATPase activity increased in concert with the increase in abundance noted in B (N=4). Values are mean ± S.E.M. *P<0.05 (one-way ANOVA, Dunnet's *post* test).

Statistics

All data are given as means ± S.E.M. Differences between groups were tested using one way analysis of variance (one-way ANOVA) or repeated-measures (RM)-ANOVA when appropriate. When RM-ANOVA was used, differences at each sampling time were tested using one-way ANOVA followed by Dunnet's *post* test, using the sham-operated or the NaCl-infused fish as the control treatment. In all cases, the fiducial level of significance was set at P<0.05.

Results
Blood parameters

Alkalotic and acidotic states were induced in the blood of the experimental fish by infusion. The blood pH of base-infused fish (BIF) increased from 7.80±0.65 to 8.21±0.26 pH units after 1 h
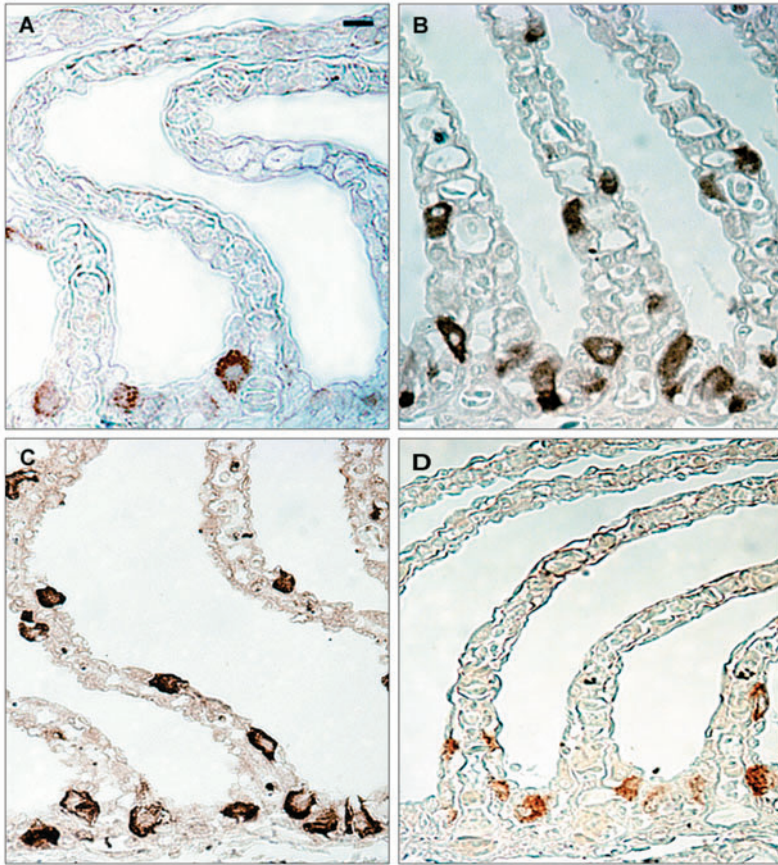
Fig. 6. Representative images of H⁺-ATPase immunostaining in gills from sham-operated (A), acid-infused (B), base-infused (C) and NaCl-infused (D) fish. The sections were from equivalent regions in the gill filament, near the trailing edge. Scale bar, 10 μm.

any experimental time. Blood haematocrit, and plasma [Na⁺], [Cl⁻] and osmolarity did not show any significant difference between the treatments or sampling times (Table 2).

Na⁺/K⁺-ATPase

Na⁺/K⁺-ATPase abundance in gill cell membranes was significantly increased after acid infusion to 315±88% of the sham-operated fish (Fig. 2A,B). However, Na⁺/K⁺-ATPase activity did not vary significantly among the treatments (Fig. 2C), a discrepancy that might be explained by the low number of samples analyzed (*N*=4). In all the treatments the number of immunolabeled cells decreased from the trailing to the leading edge region of the gill filaments, with no detectable signal in the latter. In the gill filaments from sham-operated fish and NaCl-infused fish, Na⁺/K⁺-ATPase immunolabeling was mostly found in cells of the interlamellar region, but some sections also showed extensive labeling on the lamella. In AIF and BIF, comparatively more Na⁺/K⁺-ATPase-positive cells were present higher on the lamella (Fig. 3), but it was not possible to tell if the differences were real owing to high variability in the control fish. The Na⁺/K⁺-ATPase immunostaining was restricted to the basolateral region of the cells in all the treatments, as shown in the higher magnification micrographs in Fig. 4.

H⁺-ATPase

H⁺-ATPase abundance in the membrane fraction of gills from BIF was threefold higher than in gills from the rest of the treatments, as estimated from western blots (Fig. 5A,B). The H⁺-ATPase specific activity was also significantly higher in the BIF (Fig. 5C). Similarly to Na⁺/K⁺-ATPase, the H⁺-ATPase immunoreactive signal decreased from the trailing to the leading edge region, being absent in the latter. This was the case for all the treatments. In sham-operated and NaCl-infused fish, H⁺-ATPase immunostaining was concentrated in the interlamellar region of the gills and at the base of the lamella. Qualitatively, there appear to be more H⁺-ATPase-positive cells in gill sections from AIF and BIF, especially on the lamella (Fig. 6). Control and AIF, H⁺-ATPase-positive cells showed a diffuse signal throughout the cytoplasm, slightly stronger in the apical region (Fig. 7A,B). This sub-cellular localization is similar to that previously described by Wilson et al. (1997).
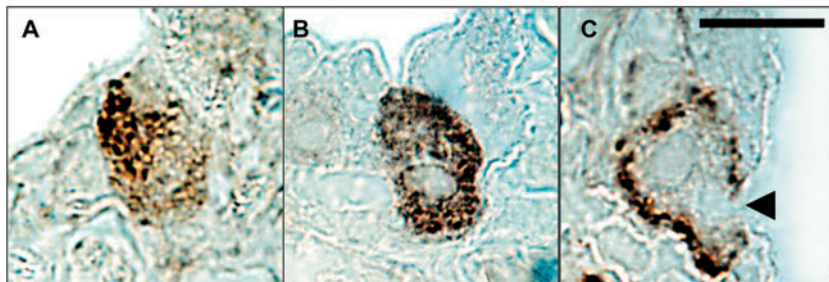
of infusion and remained elevated for the rest of the experiment. The blood pH of acid-infused fish (AIF) dropped significantly after 6 h of infusion (7.34±0.14 pH units), but recovered to control values by time *t*=12 h. The blood pH of control fish (NaCl infused) did not show significant differences throughout the experiment. These results are summarized in Fig. 1A. Total CO_2 only changed significantly in the BIF (Fig. 1B). It increased from 3.55±0.92 to 7.43±0.25 mmol l⁻¹ after 1 h, and reminded at a significantly elevated value for the rest of the experimentation period. The values for total CO_2 in the AIF were almost identical to the control, except for a transient increase at *t*=12 h (4.38±0.95 *versus* 3.03±0.21 mmol l⁻¹). However, the differences between AIF and control fish were not significant at

Fig. 7. High magnification light micrographs showing the V-H⁺-ATPase subcellular localization in control (A), acid- (B) and base-infused (C) fish. Note the distinct immunostaining at the basolateral region and the absence of staining on the apical membrane (arrowhead) in C. Scale bar, 10 μm.
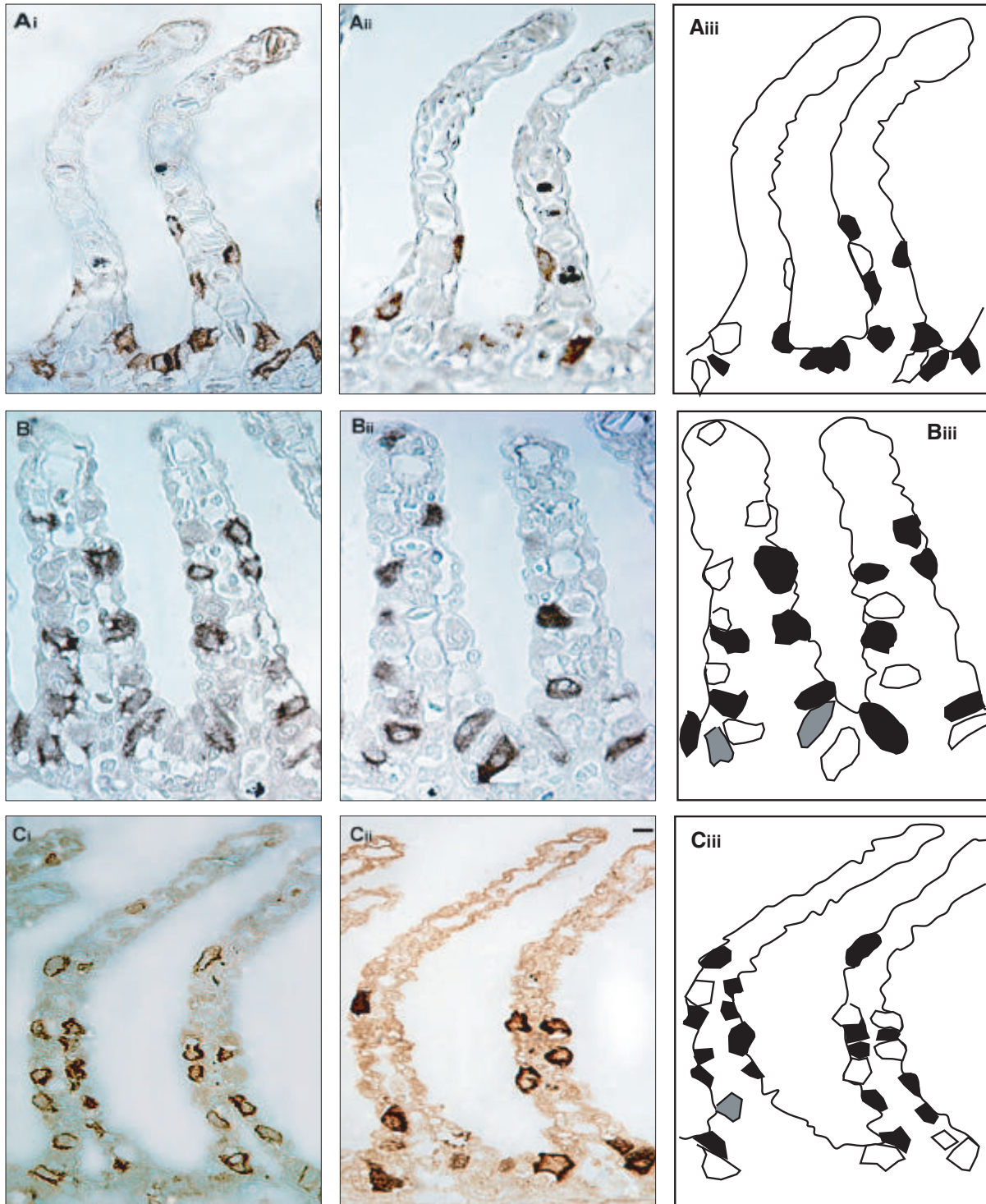
Fig. 8. Immunohistochemistry of consecutive sections from the trailing edge region of gills from sham-operated fish (A), acid-infused fish (B), and base-infused fish (C). (Ai,Bi,Ci) Na^+/K^+-ATPase immunoreactivity; (Aii,Bii,Cii) V-H^+-ATPase immunoreactivity; (Aiii,Biii,Ciii) diagrams of the approximate location of each immunostained cell. Cells that labeled positive for Na^+/K^+-ATPase only are black, those labeled for V-H^+-ATPase only are white, and cells that labeled positive for both transporters are gray. Scale bar, 10 μm.

Remarkably, the H^+-ATPase immunoreactivity in gills from BIF was distinctly confined to the basolateral region of the cells (Fig. 7C).

Colocalization of Na^+/K^+-ATPase and H^+-ATPase

Piermarini and Evans (2001) reported that in the gills of Atlantic stingray, the cells rich in Na^+/K^+-ATPase did not show
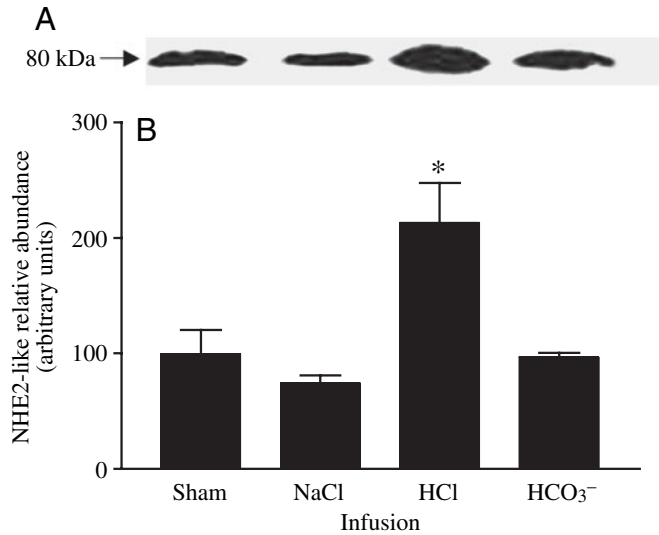
Fig. 9. Quantitative immunoblotting of the membrane fraction of gills of sham-operated, NaCl-, acid- and base-infused fish. (A) representative immunoblot incubated with anti-NHE2 antibody, showing a distinct band at ~80 kDa. (B) Fluorometric analysis showing that the abundance of NHE2 in acid infused fish was 213±5% of sham-operated fish (100±21%). $N=4$; *$P<0.05$ (one-way ANOVA, Dunnet's *post* test).

positive labeling for H$^+$-ATPase, and *vice versa*. To address this possibility in the dogfish, we incubated consecutive 4 μm sections with antibodies against either Na$^+$/K$^+$-ATPase or H$^+$-ATPase. We then identified cells in both sections and looked at the localization of the two transporters. We found only a minority of cells that were positive for both Na$^+$/K$^+$-ATPase and H$^+$-ATPase (Fig. 8). No obvious differences could be seen among the treatments.

NHE2

To determine the involvement of a NHE2-like protein in the branchial acid–base regulatory mechanism of the dogfish, we performed quantitative immunoblottings on gill membrane samples of the fish from the various treatments. All samples had a specific ~80 kDa band, but the acid-infused sample was the only one with a significantly different relative intensity (213±5% of the sham-operated fish; Fig. 9). We attempted to perform colocalization studies for Na$^+$/K$^+$-ATPase, H$^+$-ATPase and NHE2, but, unfortunately, the anti NHE2-antibody did not work for immunohistochemistry, despite trying some antigen retrievals techniques (pre treatment with 1% SDS, 10 mmol l^{-1} citric acid buffer at 97°C).

Transmission electron microscopy

We found mitochondria-rich (MR) cells in the filament and lamella of fish gills from all the treatments. The MR cell fine structure was similar to that previously reported by Laurent (1984) and Wilson et al. (2002), among others. MR cells had an ovoid appearance, with large numbers of mitochondria, long microvilli, abundant subapical vesicles and numerous basolateral membrane infoldings (Fig. 10). No qualitative
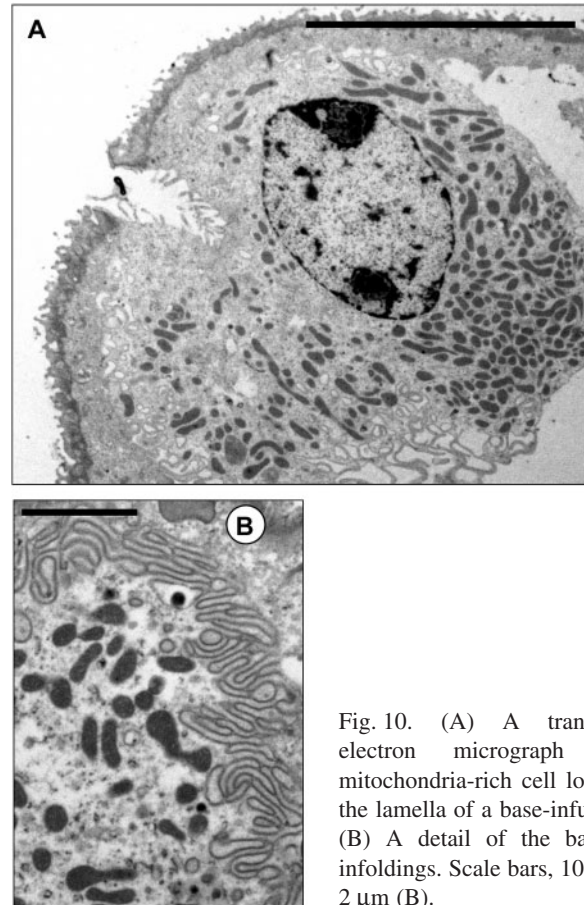

Fig. 10. (A) A transmission electron micrograph of a mitochondria-rich cell located on the lamella of a base-infused fish. (B) A detail of the basolateral infoldings. Scale bars, 10 μm (A); 2 μm (B).

differences in the ultrastructure of MR cells were found in either AIF or BIF.

Discussion

Infusions of acid and base solutions have been extensively used to study the branchial acid–base regulation in elasmobranchs. These earlier works investigated where the relevant ion fluxes take place, and their magnitude (reviewed by Heisler, 1988). Recent studies have focused on gill NH$_4^+$ excretion (Wood et al., 1995), the role of gill carbonic anhydrase (CA) in HCO$_3^-$ excretion (Swenson and Maren, 1987) or the involvement of extracellular CA in CO$_2$ excretion (Gilmour et al., 2001). To our knowledge, our study is the first to combine acid and base infusions with immunological techniques to try to elucidate the gill cellular responses to acid–base disturbances. Our conclusions are based on the assumption that the extra NaCl that is loaded into the fish blood together with the acidic and basic equivalents do not have a major effect on the gill epithelium. This assumption is based on previous research that the gills of dogfish play a minor role (if any) in net salt secretion, being clearly secondary to the rectal gland (Shuttleworth, 1988), and that removal of the rectal gland did not induce appreciable change in gill ultrastructure (Wilson et al., 2002). In the present experiment, fish infused with 500 mmol l^{-1} NaCl (NaCl-infused fish) did

not show any significant differences compared to the sham-operated fish for the variables analyzed. Since plasma osmolarity, [Na$^+$] and [Cl$^-$] remained similar to initial values throughout the infusion periods, we postulate that the extra salt load must have been handled by the rectal gland.

Blood acid–base status during infusions

The rate of acid infusion was of 495±79 μmol kg^{-1} h^{-1}. As expected, blood pH showed a tendency to drop, reaching statistical significance after 6 h of infusion, ~0.45 pH units lower than at the beginning of the experiment. However, by t=12 h blood pH had recovered to control values, where it remained until the end of the infusions. Moreover, we also found a transient, although not statistically significant, increase in blood total CO_2 at t=12 h. Put together, this suggests an augmentation in the capacity for acid excretion and HCO_3^- reabsorption after 6 h of continuous acid-loading due to increased expression of proteins involved in these mechanisms. Nevertheless, we cannot rule out a contribution of intracellular buffering and net H$^+$ transfer into this compartment as a potential mechanism for regulation of extracellular pH independently of branchial ionic transfers. This is a question that will form the basis for further experimentation.

HCO_3^- was infused at an even higher rate, roughly twice as much as H$^+$ (981±235 μmol kg^{-1} h^{-1}; the rationale for the mismatch is explained in the Materials and methods) producing immediate increases in blood pH and in plasma total CO_2. By t=6 and t=24 h these parameters equilibrated at ~8.0 pH units and 10 mmol l^{-1} CO_2, suggesting that a new steady state status was reached by increased by HCO_3^- secretion and/or H$^+$ reabsorption.

The magnitude of the acid–base disturbances induced by our infusions is severe. However, even greater drops in the blood pH of dogfish have been reported to occur in situations such as exhaustive exercise (Richards et al., 2003) and environmental hypercapnia (Claiborne and Evans, 1992). Similarly, unpublished results by C. Wood, M. Kajimura, T. Mommsen and P. Walsh show that arterial blood pH increases significantly between 3 h and 9 h after feeding. In their study, arterial pH peaked at 8.1 compared to control conditions of 7.9 pH units, values very similar to those obtained in our study.

Ion transporting cell subtypes

The immunostained sections suggest that there are at least two potential subpopulations of ion-transporting cells in the gills of the dogfish: H$^+$-ATPase-rich cells and Na$^+$/K$^+$-ATPase-rich cells, whose roles in acid–base regulation are discussed below. These findings are in agreement with previous research in the Atlantic stingray by Piermarini and Evans (2001), who similarly found independent H$^+$-ATPase- and Na$^+$/K$^+$-ATPase-rich cells in the gills. In contrast, we also found a small proportion of cells that labeled positive for both transporters. However, this result must be treated with caution, since these cells may either represent a true subpopulation of cells carrying the two transporters or may represent an artifact of using two antibodies on consecutive sections. Regardless, the relatively

small proportion of double-labeled cells likely indicates that, if they represent a true subtype, their role in the branchial acid–base regulation in the dogfish would be of minor importance compared to either the H$^+$-ATPase- or Na$^+$/K$^+$-ATPase-rich cells.

Acid secretion

It is generally accepted that the primary gill acid-secretory mechanism in marine fish involves apical Na$^+$/H$^+$ exchange through specialized gill cells. This hypothesis is based on the inward directed Na$^+$ gradient that fish face in seawater, which could drive acid secretion, and supported by several studies that show the presence of either NHE2- and/or NHE3-like proteins in the gills of hagfish (Choe et al., 2002), squaliform, myliobatiform and rajiform elasmobranchs (Choe et al., 2002; Edwards et al., 2002) and a variety of teleosts (Claiborne et al., 1999; Choe et al., 2002; Wilson et al., 2000a). The increase in NHE2 abundance in our acid-infused fish is evidence for the involvement of this protein in branchial acid secretion in the dogfish. Unfortunately, we were unable to detect its cellular localization as immunohistochemical analysis was not possible. However, based on numerous studies in both mammalian tissue (see Féraille and Doucet, 2001) and in other marine fishes (Claiborne et al., 2002; Edwards et al., 2002; Wilson et al., 2000a), we propose that NHE2 in dogfish is also localized on the apical membrane of polarized epithelial cells rich in Na$^+$/K$^+$-ATPase. Supporting this theory, we found an increase in abundance of the α-subunit of the Na$^+$/K$^+$-ATPase after acid infusion, suggesting that Na$^+$/K$^+$-ATPase is involved in powering electroneutral apical Na$^+$/H$^+$ by secondary active transport. In order for this hypothesis to be tested, the generation of specific antibodies for dogfish NHE2 is imperative.

Another mechanism to increase net branchial H$^+$ secretion could be to use a V-type H$^+$-ATPase located on the apical membrane. While we found an increased number of H$^+$-ATPase-rich cells on the lamella of AIF, H$^+$-ATPase abundance and activity in gill membrane fractions remained unchanged compared to the control fish. This apparent contradiction could be due to the fact that H$^+$-ATPase in AIF and control fish is mainly located on cytoplasmic vesicles. Our assays for activity and quantity involved differential centrifugation that loses the cytoplasmic fraction, which may explain the discrepancy in our current findings. At this point it is worth noting that using H$^+$-ATPases to extrude protons to seawater – a hypernatric and typically alkaline milieu – seems to be an energetically less convenient alternative than electroneutral Na$^+$/H$^+$ exchange. Regardless, we do see an apparent increase in the number of H$^+$-ATPase-positive cells after acid infusion, the reasons for this increase remain obscure. It is thus possible that both mechanisms (NHE2 and H$^+$-ATPase) contribute to acid secretion, as in the proximal tubule and thick ascending limb of the mammalian kidney (reviewed by Gluck and Nelson, 1992).

Base secretion

The samples from the BIF showed an increase in all three

of the variables related to H⁺-ATPase tested. Although no statistical analysis was performed, it was apparent that more H⁺-ATPase-rich cells were located on the lamella and on the gill filament of BIF than of control fish, together with a significantly higher H⁺-ATPase abundance and activity in gill membranes. The immunostained sections provided further information regarding the involvement of H⁺-ATPase in base secretion. In contrast with the rest of the treatments, H⁺-ATPase was distinctly confined to the basolateral region of gill cells in the BIF. To compensate for an alkalosis, excess HCO_3^- would need to be secreted by the gills and/or H⁺ retained within the body. We believe that H⁺-ATPases are inserted in the basolateral membrane under alkalotic stress and function to rid the cell of excess H⁺ generated by hydration of CO_2 by intracellular CA, which is present in dogfish gills (Swenson and Maren, 1987; Wilson et al., 2000b). Furthermore, when gill intracellular CA was selectively blocked in fish made alkalotic by $NaHCO_3$ infusion, there was a significant reduction of HCO_3^- secretion (Swenson and Maren, 1987), suggesting an involvement in acid–base regulation via an apical anion exchange. Current research in our lab is focused on elucidating the identity of the apical anion exchanger. By analogy to the Atlantic stingray (Piermarini et al., 2002), the most promising lead points to a pendrin-like protein.

In summary, we have established the presence of at least two types of ion-transporting cells, Na⁺/K⁺-ATPase- and H⁺-ATPase-rich cells in the gills of a marine stenohaline elasmobranch. Based on responses to acid and base infusions, we propose that a NHE2-like protein participates in acid secretion, and that basolateral V-H⁺-ATPases are involved in net base secretion.

References

Brown, D. and Breton, S. (1996). Mitochondria-rich, proton-secreting epithelial cells. *J. Exp. Biol.* **199**, 2345-2358.

Choe, K. P., Morrison-Shetlar, A. I., Wall, B. P. and Claiborne, J. B. (2002). Immunological detection of Na⁺/H⁺ exchangers in the gills of a hagfish, *Myxine glutinosa*, an elasmobranch, *Raja erinacea*, and a teleost, *Fundulus heteroclitus*. *Comp. Biochem. Physiol.* **131A**, 375-385.

Claiborne, J., Blackston, C., Choe, K., Dawson, D., Harris, S., Mackenzie, L. and Morrison-Shetlar, A. (1999). A mechanism for branchial acid excretion in marine fish: identification of multiple Na⁺/H⁺ antiporter (NHE) isoforms in gills of two seawater teleosts. *J. Exp. Biol.* **202**, 315-324.

Claiborne, J. B., Edwards, S. L. and Morrison-Shetlar, A. I. (2002). Acid-base regulation in fishes: cellular and molecular mechanisms. *J. Exp. Zool.* **293**, 302-319.

Claiborne, J. B. and Evans, D. H. (1992). Acid-base balance and ion transfers in the spiny dogfish (Squalus acanthias) during hypercapnia: a role for ammonia excretion. *J. Exp. Zool.* **261**, 9-17.

Edwards, S. L., Donald, J. A., Toop, T., Donowitz, M. and Tse, C. M. (2002). Immunolocalisation of sodium/proton exchanger-like proteins in the gills of elasmobranchs. *Comp. Biochem. Physiol.* **131A**, 257-265.

Féraille, E. and Doucet, A. (2001). Sodium-potassium-adenosinetriphosphatase-dependent sodium transport in the kidney: hormonal control. *Physiol. Rev.* **81**, 345-418.

Gilmour, K. M., Perry, S. F., Bernier, N. J., Henry, R. P. and Wood, C. M. (2001). Extracellular carbonic anhydrase in the dogfish, *Squalus acanthias*: a role in CO_2 excretion. *Physiol. Biochem. Zool.* **74**, 477-492.

Gluck, S., Nelson, R., Lee, B., Wang, Z., Guo, X., Fu, J. and Zhang, K. (1992). Biochemistry of the renal V-ATPase. *J. Exp. Biol.* **172**, 219-229.

Hawkings, G. S., Galvez, F. and Goss, G. G. (2004). Seawater acclimation causes independent alterations in Na⁺/K⁺- and H⁺-ATPase activity in isolated mitochondria-rich cell subtypes of the rainbow trout gill. *J. Exp. Biol.* **207**, 905-912.

Heisler, N. (1988). Acid–base regulation. In *Physiology of Elasmobranch Fishes* (ed. T. J. Shuttleworth), pp. 215-252. Berlin: Springer-Verlag.

Katoh, F., Hyodo, S. and Kaneko, T. (2003). Vacuolar-type proton pump in the basolateral plasma membrane energizes ion uptake in branchial mitochondria-rich cells of killifish *Fundulus heteroclitus*, adapted to a low ion environment. *J. Exp. Biol.* **206**, 793-803.

Katoh, F. and Kaneko, T. (2003). Short-term transformation and long-term replacement of branchial chloride cells in killifish transferred from seawater to freshwater, revealed by morphofunctional observations and a newly established 'time-differential double fluorescent staining' technique. *J. Exp. Biol.* **206**, 4113-4123.

Katoh, F., Shimizu, A., Uchida, K. and Kaneko, T. (2000). Shift of chloride cell distribution during early life stages in seawater-adapted killifish, *Fundulus heteroclitus*. *Zool. Sci.* **17**, 11-18.

Kirschner, L. B. (2004). The mechanism of sodium chloride uptake in hyperregulating aquatic animals. *J. Exp. Biol.* **207**, 1439-1452.

Laemmli, U. K. (1970). Cleavage of structural proteins during the assembly of the head of the bacteriophage T4. *Nature* **227**, 680-685.

Laurent, P. (1984). Gill internal morphology. In *Fish Physiology*, vol. 10A eds H. W. S. and D. W. Randall), pp. 73-183. New York: Academic Press.

McCormick, S. D. (1993). Methods for non-lethal gill biopsy and measurements of Na⁺/K⁺-ATPase activity. *Can. J. Fish Aquat. Sci.* **50**, 656-658.

Piermarini, P. M. and Evans, D. H. (2001). Immunochemical analysis of the vacuolar proton-ATPase B-subunit in the gills of a euryhaline stingray (*Dasyatis sabina*): effects of salinity and relation to Na⁺/K⁺-ATPase. *J. Exp. Biol.* **204**, 3251-3259.

Piermarini, P. M., Verlander, J. W., Royaux, I. E. and Evans, D. H. (2002). Pendrin immunoreactivity in the gill epithelium of a euryhaline elasmobranch. *Am. J. Physiol.* **283**, R983-R992.

Richards, J., Heigenhauser, G. and Wood, C. (2003). Exercise and recovery metabolism in the Pacific spiny dogfish (*Squalus acanthias*). *J. Comp. Physiol.* **173B**, 463-474.

Shuttleworth, T. J. (1988). Salt and water balance-extrarenal mechanisms. In *Physiology of Elasmobranch Fishes* (ed. T. J. Shuttleworth), pp. 171-199. Berlin: Springer-Verlag.

Swenson, E. R. and Maren, T. H. (1987). Roles of gill and red cell carbonic anhydrase in elasmobranch HCO_3^- and CO_2 excretion. *Am. J. Physiol.* **253**, R450-R458.

Wilson, J. M., Morgan, J. D., Vogl, A. W. and Randall, D. J. (2002). Branchial mitochondria-rich cells in the dogfish *Squalus acanthias*. *Comp. Biochem. Physiol.* **132A**, 365-374.

Wilson, J., Randall, D., Donowitz, M., Vogl, A. and Ip, A. (2000a). Immunolocalization of ion-transport proteins to branchial epithelium mitochondria-rich cells in the mudskipper (*Periophthalmodon schlosseri*). *J. Exp. Biol.* **203**, 2297-2310.

Wilson, J. M., Randall, D. J., Vogl, A. W., Harris, J., Sly, W. S. and Iwama, G. K. (2000b). Branchial carbonic anhydrase is present in the dogfish, *Squalus acanthias*. *Fish Physiol. Biochem.* **22**, 329-336.

Wilson, J. M., Randall, D. J., Vogl, A. W. and Iwama, G. K. (1997). Immunolocalization of proton-ATPase in the gills of the elasmobranch, *Squalus acanthias*. *J. Exp. Zool.* **278**, 78-86.

Wood, C. M., Part, P. and Wright, P. A. (1995). Ammonia and urea metabolism in relation to gill function and acid-base balance in a marine elasmobranch, the spiny dogfish (*Squalus acanthias*). *J. Exp. Biol.* **198**, 1545-1558.

Zall, D. M., Fischer, M. D. and Garner, Q. M. (1956). Photometric determination of chloride in water. *Anal. Chem.* **28**, 1665-1678.